

Development of a new dynamic procedure for the Clark model of the subgrid-scale scalar flux using the concept of optimal estimator

Y. Fabre and G. Balarac

Grenoble-INP/CNRS/UJF-Grenoble 1, LEGI UMR 5519, Grenoble, F-38041, France

(Received 8 April 2011; accepted 8 October 2011; published online 9 November 2011)

Accurate prediction of a scalar advected by a turbulent flow is needed for various applications. In the framework of large-eddy simulation (LES), an accurate subgrid-scale (SGS) model for the subgrid-scale scalar flux has to be used. In this work, the performance of various dynamic SGS models is first evaluated by *a priori* tests through the concept of optimal estimator. Direct numerical simulation (DNS) in homogeneous isotropic turbulence is performed on 512^3 grid points. Filtered quantities are extracted from the DNS data using a box or a spectral cut-off filter. The models' accuracy is then evaluated in term of structural and functional performances, i.e., the model capacity to locally approximate the SGS unknown term and to reproduce its energetic action, respectively. It is shown that the Clark model has the best set of parameters to describe the SGS scalar flux. However, the classic dynamic procedure usually applied to compute the model coefficient leads to a large error. A new dynamic procedure is thus proposed to reduce this error. The results show that the new dynamic model leads to a good accuracy, which is not expectable from a model based only on the parameters of the classic dynamic Smagorinsky model. To better evaluate the improvement of the new dynamic procedure, *a posteriori* (large-eddy simulation) tests are performed for three different Schmidt numbers. It is shown that the new model allows to improve substantially the prediction of various scalar statistics. © 2011 American Institute of Physics. [doi:10.1063/1.3657090]

I. INTRODUCTION

Various applications need to solve a scalar equation simultaneously to the governing flow equations. In these applications, the scalar can represent the temperature field or the concentration of chemical species in combustion, mixing, or heat transfer studies. Due to the large range of motion scales in turbulent flows, the direct numerical simulation (DNS) of realistic applications is not yet available because of the important computational cost. To overcome this limitation, the large-eddy simulation (LES) technique proposes to explicitly solve only the large scales of the flow and to model the smallest scales. This separation between resolved large scales and modeled small scales is performed by a filtering operation,

$$\bar{f}(\vec{x}, t) = \int f(\vec{y}, t) G(\vec{x} - \vec{y}) d\vec{y}, \quad (1)$$

to obtain the large-scale resolved field, \bar{f} , from the turbulent field, f , with G the filter kernel. This filtering operation applied to the flow equations leads to subgrid-scale (SGS) terms which have to be modeled. While many SGS models have been designed to close the filtered Navier-Stokes equations for incompressible flows,¹⁻³ the corresponding problem for the scalar equation has not yet been fully addressed. For example, recent works^{4,5} have shown a dependence of the SGS scalar modeling with the molecular Schmidt number, $Sc = \nu/D$, where ν and D represent the molecular viscosity and the molecular diffusivity, respectively. The filtered transport equation for a passive scalar, Z , in incompressible flow is given by

$$\frac{\partial \bar{Z}}{\partial t} + \bar{u}_i \frac{\partial \bar{Z}}{\partial x_i} = D \frac{\partial^2 \bar{Z}}{\partial x_i^2} - \frac{\partial T_i}{\partial x_i}, \quad (2)$$

where $T_i = \overline{u_i Z} - \bar{u}_i \bar{Z}$ is the SGS scalar flux, which has to be modeled to perform LES. An eddy diffusivity, D_T , is commonly introduced to model the SGS scalar flux as $T_i = D_T \partial \bar{Z} / \partial x_i$. In the simplest models, the eddy diffusivity is defined from the eddy viscosity, ν_T , through a constant eddy Schmidt number,^{6,7} $Sc_T = \nu_T / D_T \approx 0.6$. However, Moin *et al.*⁸ introduce a Smagorinsky-type model with a dynamic procedure to compute the model coefficient. They show that the dynamic procedure greatly improves the results of the simulations and leads to a non-constant value of Sc_T , since the eddy diffusivity depends on the molecular Schmidt number and on the local turbulence level of the flow. Even if a correct dissipation level is modeled, the Smagorinsky-type models are generally known to have a weak correlation between the model and the SGS term.⁹ To overcome this behavior, the concept of the Clark model consists in adding a gradient model (GM) to the Smagorinsky-type model to obtain both the relatively accurate representation of the SGS term by the gradient model and a proper dissipation provided by the Smagorinsky-type model.⁹ A dynamic procedure can then be applied to define a dynamic Clark model (DCM).¹⁰

In this work, we first study the performance of the dynamic Smagorinsky-type model (DSM) and the dynamic Clark model in term of structural and functional performances through *a priori* tests. It is shown that the dynamic Clark model is the best candidate to model T_i . However, a gap persists between the measured performance and the optimal performance expected for this model. To improve the results of

the Clark model, a new dynamic procedure is proposed. The new dynamic Clark model (NDCM) is then tested in a *posteriori* (LES) tests. From the LES performed, it is shown that the new model substantially improves the prediction of various scalar statistics in comparison with the dynamic Smagorinsky-type and the classic dynamic Clark model.

II. NUMERICAL METHOD

In the first part of this work, *a priori* tests are performed. The data are extracted from DNS of forced homogeneous isotropic turbulence. A pseudo-spectral code with second-order explicit Runge-Kutta time-advancement is used. The viscous terms are treated exactly. The simulation domain is discretized using 512^3 grid points on a domain of length 2π . A classic 3/2 rule is used for dealiasing the non-linear convection term, and statistical stationarity is achieved using a forcing term.¹¹ The scalar equation is advanced simultaneously using an identical numerical scheme. The scalar field is initialized between 0 and 1 according to the procedure proposed by Eswaran and Pope.¹² To be sure to simulate all the dissipative scales of the turbulence,¹³ parameters are chosen such that $k_{\max}\eta > 1.5$ and $k_{\max}\eta_B > 1.5$, where k_{\max} is the maximal wavenumber in the box, and η and η_B are the Kolmogorov and Batchelor scales, respectively. The Schmidt number is taken equal to 1.0 and the Reynolds number based on the Taylor microscale is around 180 at the stationary state. The code and the flow configuration are similar to previous works where the modeling of the SGS scalar variance and the SGS scalar dissipation rate^{14–16} were studied.

In *a priori* tests, the DNS data are filtered in space to emulate LES quantities. Two different filters are used. The box filter is first used to replicate the implicit filter associated with discretization methods often used in LES of engineering flow, such as centered finite difference scheme¹⁷ or finite volume method.¹⁸ The spectral cut-off filter is also used to reproduce the behavior of the spectral method employed in this work. Several filter sizes have been used chosen as $2 \leq \bar{\Delta}/\Delta x \leq 16$, where $\bar{\Delta}$ is the filter width and Δx is the DNS mesh size. Figure 1 shows the scalar variance spectrum with the location of the filters in the wavenumber space.

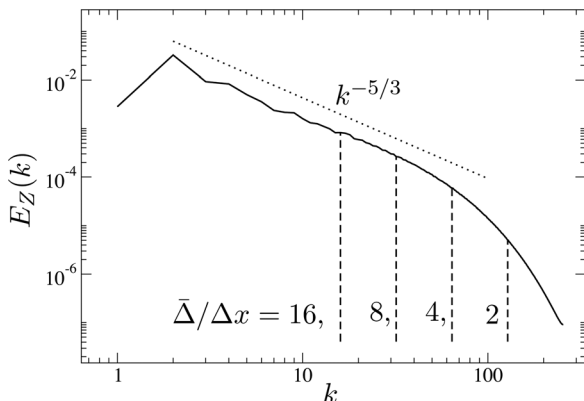


FIG. 1. Scalar variance spectrum, $E_Z(k)$, with the location of the filters used in this work.

III. MEASUREMENTS OF THE MODELS PERFORMANCE

First, the DNS data are used to measure the performance of SGS scalar flux models. The most commonly used model is the DSM proposed by Moin *et al.*⁸ In this model, the eddy diffusivity is defined similarly to the Smagorinsky eddy viscosity model.¹⁹ The SGS scalar flux is thus defined as

$$T_i = \overline{u_i Z} - \bar{u}_i \bar{Z} = C_d \bar{\Delta}^2 |\bar{S}| \frac{\partial \bar{Z}}{\partial x_i}, \quad (3)$$

where $|\bar{S}| = (2\bar{S}_{ij}\bar{S}_{ij})^{1/2}$, with $\bar{S}_{ij} = 1/2(\partial\bar{u}_i/\partial x_j + \partial\bar{u}_j/\partial x_i)$ the filtered strain rate tensor. The model coefficient C_d is determined dynamically using the Germano identity.^{20,21} This procedure uses a test filter, noted $\hat{\cdot}$, defined similarly to the first one. The test filter width, noted $\hat{\Delta}$, is taken such as $\hat{\Delta} = 2\bar{\Delta}$. As first step, the dynamic procedure consists to apply the test filter to Eq. (3) leading to

$$\widehat{\overline{u_i Z}} - \widehat{\bar{u}_i \bar{Z}} = C_d \bar{\Delta}^2 |\bar{S}| \frac{\partial \bar{Z}}{\partial x_i}, \quad (4)$$

assuming that the coefficient C_d varies slowly in space. The second step is to assume the same model coefficient when the model (2) is written for the combination of both filters, noted $\hat{\cdot}$, leading to

$$\widehat{\overline{u_i Z}} - \hat{u}_i \hat{Z} = C_d \hat{\Delta}^2 |\hat{S}| \frac{\partial \hat{Z}}{\partial x_i}, \quad (5)$$

where $\hat{\Delta}$ is the width of the filter given by the composition of both filters. Vreman *et al.*¹⁰ show $\hat{\Delta} = \sqrt{5}\bar{\Delta}$ for a Gaussian filter. They also explain that the combination of two box filters is a “trapezoid” filter. However, it can be well approximated by a box filter with the same relation than above. The spectral cut-off filter being idempotent, there is $\hat{\Delta} = \bar{\Delta}$. However, $\hat{\Delta} = \bar{\Delta}$ is often assumed independently of the filter used. The influence of this assumption when a box filter is used will be investigated below when the performance of the dynamic Smagorinsky-type model will be measured. Finally, subtracting Eq. (4) from Eq. (5) provides

$$L_i = C_d M_i, \quad (6)$$

with

$$L_i = \widehat{\overline{u_i Z}} - \hat{u}_i \hat{Z} \quad (7)$$

and

$$M_i = \hat{\Delta}^2 |\hat{S}| \frac{\partial \hat{Z}}{\partial x_i} - \bar{\Delta}^2 |\bar{S}| \frac{\partial \bar{Z}}{\partial x_i}. \quad (8)$$

Assuming that the coefficient is constant over homogeneous directions, C_d is then obtained with a least-squares averaging procedure²¹

$$C_d = \frac{\langle L_i M_i \rangle}{\langle M_i M_i \rangle}, \quad (9)$$

where the brackets indicate a statistical average over homogeneous directions of the flow. Note that, in the case of

homogeneous isotropic turbulence, C_d is constant in the whole domain. The dynamic Smagorinsky-type model is very popular since the few number of needed parameters makes it easy to implement, and since the dynamic computation of the model coefficient highly improves the accuracy in shear flow regions by reducing the over-dissipation. However, it is known that SGS models only based on an eddy diffusivity assumption lead to weak correlations between the model and the SGS term.⁹ To improve the model, it has been proposed to combine the Smagorinsky-type model with a more accurate representation of the SGS term.⁹ This approach defines the Clark model written as

$$T_i = \overline{u_i \bar{Z}} - \bar{u}_i \bar{Z} = \frac{\bar{\Delta}^2}{12} \frac{\partial \bar{u}_i}{\partial x_j} \frac{\partial \bar{Z}}{\partial x_j} + C_c \bar{\Delta}^2 |\bar{S}| \frac{\partial \bar{Z}}{\partial x_i}. \quad (10)$$

The first term of the right-hand-side (RHS) defines the gradient model. This model is known to lead to very high correlations with the SGS term but not to provide enough energy transfer between grid scales and subgrid-scales. This leads to unstable simulations when this model is used without an additional eddy-diffusivity part.¹⁰ In Eq. (10), C_c is the model coefficient. Adapting the Germano procedure, C_c can be determined from the following relation:

$$L_i = C_c M_i + H_i, \quad (11)$$

where L_i and M_i are always defined by Eq. (7) and Eq. (8), respectively, and where H_i is a new term coming from the gradient part of the model,

$$H_i = \frac{\hat{\Delta}^2}{12} \frac{\partial \hat{u}_i}{\partial x_j} \frac{\partial \hat{Z}}{\partial x_j} - \frac{\bar{\Delta}^2}{12} \frac{\partial \bar{u}_i}{\partial x_j} \frac{\partial \bar{Z}}{\partial x_j}. \quad (12)$$

Assuming that the coefficient is constant over homogeneous directions, C_c is also obtained with a least-squares averaging procedure

$$C_c = \frac{\langle (L_i - H_i) M_i \rangle}{\langle M_i M_i \rangle}. \quad (13)$$

The DCM is thus defined.

To better understand the advantage of using the DCM instead of the DSM, the performance of each model is measured from *a priori* tests. As already explained a box and a spectral cut-off filters are used to reproduce the behavior of centered finite differences and of spectral methods, respectively. The models' performances are analyzed in terms of structural and functional performances.³ The structural performance is defined as the model ability to describe locally the SGS unknown term appearing in the resolved equation. For the scalar, the SGS unknown term is the divergence of the SGS scalar flux, $\partial T_i / \partial x_i$, appearing in the scalar transport equation (2). In the framework of optimal estimation theory,²² the models structural performance is first evaluated using the notion of an optimal estimator recently introduced by Moreau *et al.*²³ in the LES context. The starting point of this idea is to define the quadratic error,

$$\epsilon_Q = \langle (f - g(\phi))^2 \rangle, \quad (14)$$

as the relevant error to consider in LES.²⁴ In this definition, f is the SGS term to model and g is a model of f based on a given set of variables ϕ . The brackets indicate a statistical average over a suitable ensemble. The concept of optimal estimator forecasts that any model g built on the set of variables ϕ will lead to a quadratic error higher than a minimal value. This minimal value is achieved when the model g is equal to $\langle f | \phi \rangle$, the expectation of the exact quantity f conditioned with the set of variables ϕ . The quantity $\langle f | \phi \rangle$ is then defined as the optimal estimator of f for the set of variable ϕ . The error based on this optimal estimator, noted ϵ_{irr} , is defined such as

$$\epsilon_{irr} = \langle (f - \langle f | \phi \rangle)^2 \rangle \leq \epsilon_Q. \quad (15)$$

It is called the irreducible error since no model using only ϕ as set of variables can lead to a smaller error. The optimal estimator theory allows to provide various informations on the SGS models used in LES. First we can evaluate the quadratic error of each model to see which one gives the best results in modelling the SGS unknown term. The most suitable set of variables to model the SGS term can also be determined by comparing the irreducible error of different models. The set of variables with the smallest irreducible error will be the best candidate to design a model. Finally, the improvement possibility of a given model can be determined. Indeed, if the quadratic error of a given model is much higher than its irreducible part, improvement can be expected (by modification of the coefficient computation, for example). This concept has already been used to improve the modeling of SGS quantities needed for LES of combustion.^{14,15}

Figure 2 shows the evolution with the filter width of the normalized quadratic and irreducible errors of DSM and DCM on the modeling of $\partial T_i / \partial x_i$, for the box and the spectral cut-off filter. In the following, the error computations are always normalized by the statistical variance of the exact SGS term. For DSM, the set of variables used to compute the irreducible error is $\left\{ \frac{\partial}{\partial x_i} \left(|\bar{S}| \frac{\partial \bar{Z}}{\partial x_j} \right) \right\}$, whereas the DCM set of variables is $\left\{ \frac{\partial}{\partial x_i} \left(\frac{\partial \bar{u}_i}{\partial x_j} \frac{\partial \bar{Z}}{\partial x_j} \right), \frac{\partial}{\partial x_i} \left(|\bar{S}| \frac{\partial \bar{Z}}{\partial x_j} \right) \right\}$. On this figure, the errors of the GM defined only with the first term of the RHS in Eq. (10) is also added for comparison. For this model, the set of variables is $\left\{ \frac{\partial}{\partial x_i} \left(\frac{\partial \bar{u}_i}{\partial x_j} \frac{\partial \bar{Z}}{\partial x_j} \right) \right\}$. First conclusions can then be addressed. As expected, for both filter used, the quadratic error of the structural models (DCM and GM) are smaller than DSM quadratic error, showing that these models have better structural performances. Moreover, the DCM and GM quadratic errors are smaller than the DSM irreducible error. This shows that the improvement of the structural performance of DSM cannot be expected without adding new quantities in its set of variables. Finally, since the DCM irreducible error is the smallest one, it appears that the DCM set of variables is the best candidate to model $\partial T_i / \partial x_i$. However, the DCM quadratic error is significantly larger than its associated irreducible error, in particular, for large filter sizes. These results show that a better model can potentially be

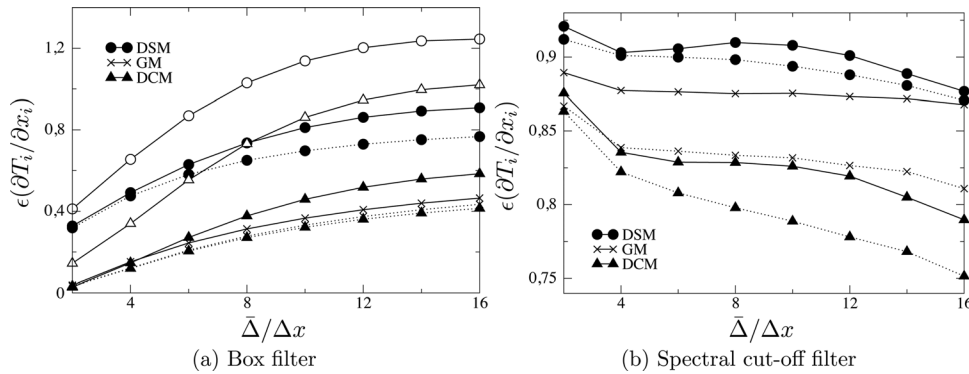


FIG. 2. Evolution of the quadratic errors (solid line) of the models on the prediction of $\partial T_i/\partial x_i$ and their associated irreducible errors (dotted line) with the filter width. For the box filter, the results are shown for the dynamic procedure using $\hat{\Delta} = \sqrt{5}\bar{\Delta}$ (solid symbols) and using $\hat{\Delta} = \bar{\Delta}$ (open symbols).

formulated with the same set of variables, but that a substantial improvement is needed to achieve this goal. Note that, in the case of the box filter (Fig. 2(a)), the quadratic errors of the dynamic models are computed for the exact value $\hat{\Delta} = \sqrt{5}\bar{\Delta}$ and for the commonly used approximation $\hat{\Delta} = \bar{\Delta}$. It is thus shown that the approximation $\hat{\Delta} = \bar{\Delta}$ leads to an important deterioration of the structural performance of the dynamic models with an important growth of the quadratic errors.

The models performances are now evaluated in term of functional performance. The functional performance represents the ability of the model to reproduce the action of the SGS term on the transported quantity (here, the scalar field) and not the term itself.³ In the scalar case, the action of the SGS term is to allow the transfer between the resolved scalar “energy,” \bar{Z}^2 , and the SGS scalar variance, $\overline{\bar{Z}Z} - \bar{Z}\bar{Z}$. From the transport equation of \bar{Z}^2 ,

$$\frac{\partial \bar{Z}^2}{\partial t} + \bar{u}_i \frac{\partial \bar{Z}^2}{\partial x_i} = D \frac{\partial^2 \bar{Z}^2}{\partial x_i^2} - 2D \frac{\partial \bar{Z}}{\partial x_i} \frac{\partial \bar{Z}}{\partial x_i} - 2 \frac{\partial \bar{Z} T_i}{\partial x_i} + 2 T_i \frac{\partial \bar{Z}}{\partial x_i}, \quad (16)$$

it appears that this transfer is controlled by the SGS scalar dissipation, $T_i \partial \bar{Z} / \partial x_i$. The functional performance will thus be defined as the model capacity to accurately evaluate this term. To estimate the models functional performance, the optimal estimation theory can be used. The quadratic and the irreducible errors are now defined for the modeling of the SGS scalar dissipation, $T_i \partial \bar{Z} / \partial x_i$. Figure 3 shows the evolution with the filter width of these quadratic and irreducible errors. Since the DCM irreducible error is still the smallest error, the DCM set of variables appears as the best candidate to evaluate the SGS scalar dissipation. However, the DCM

quadratic error can be very important and even higher than the DSM quadratic error when a spectral cut-off filter is used. This shows a poor functional performance for DCM. This confirms that an efficient model can potentially be formulated with the DCM variables set, whereas it cannot be expected with the DSM model. As expected, the GM performance is deteriorated with the filter width growth. Indeed, the gradient model was defined from the first term of a Taylor series expansion used to approximate the filtering operation.²⁵ However, for high filter sizes, the other terms are no more negligible.

The functional performance is also studied from the evolution of the mean SGS scalar dissipation, $\langle T_i \partial \bar{Z} / \partial x_i \rangle$. Figure 4 shows the results for the box and spectral cut-off filters. The mean SGS scalar dissipation, $\langle T_i \partial \bar{Z} / \partial x_i \rangle$, is negative showing that the transfers are from the large (resolved) scales to the small ones. First, it is shown that GM under-predicts the magnitude of $\langle T_i \partial \bar{Z} / \partial x_i \rangle$ in comparison with the DNS results. This is the well-known problem for this model. Indeed, this model is known to not provide enough dissipation, leading to unstable simulations.²⁶ Conversely, the other models are too dissipative with an over-prediction of the magnitude of $\langle T_i \partial \bar{Z} / \partial x_i \rangle$. DCM is even more dissipative than DSM. It confirms that the DCM functional performance is weak. Note that for the box filter, Figures 3(a) and 4(a) also show the results when the approximation $\hat{\Delta} = \bar{\Delta}$ is done to compute the dynamic coefficient. Again, it is shown that this approximation deteriorates the dynamic models performance with a growth of the quadratic error associated to a large over-prediction of the magnitude of $\langle T_i \partial \bar{Z} / \partial x_i \rangle$. These results show the importance of using $\hat{\Delta} = \sqrt{5}\bar{\Delta}$ for the dynamic procedure when a box filter is used. In the following, the dynamic procedure using $\hat{\Delta} = \bar{\Delta}$ for the box filter will no more be considered.

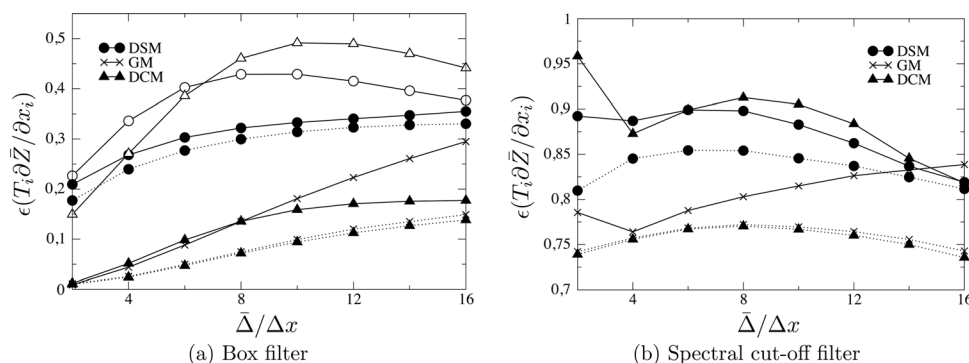


FIG. 3. Evolution of the quadratic errors (solid line) of the models on the prediction of $T_i \partial \bar{Z} / \partial x_i$ and their associated irreducible errors (dotted line) with the filter width. For the box filter, the results are shown for the dynamic procedure using $\hat{\Delta} = \sqrt{5}\bar{\Delta}$ (solid symbols) and using $\hat{\Delta} = \bar{\Delta}$ (open symbols).

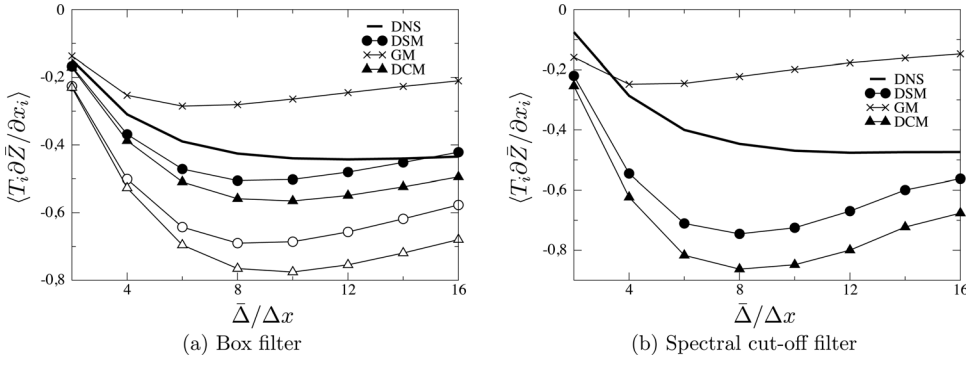


FIG. 4. Evolution of the mean SGS scalar dissipation, $\langle T_i \partial \bar{Z} / \partial x_i \rangle$, with the filter width. For the box filter, the results are shown for the dynamic procedure using $\hat{\Delta} = \sqrt{5} \bar{\Delta}$ (solid symbols) and using $\hat{\Delta} = \bar{\Delta}$ (open symbols).

This analyze based on the concept of optimal estimator theory allows to show that the irreducible error of DSM is generally higher than the quadratic error of the other models for both functional and structural performances (Figs. 2 and 3). Since the irreducible error represents the smallest possible error for a given set of parameters, this shows that an improvement of the modeling performance for the Smagorinsky-type model cannot be expected. Conversely, the irreducible error of DCM is the smallest irreducible error. However, the DCM quadratic error can be significantly larger than its irreducible part for both functional and structural performances. This shows that an improvement of the modeling performance can be obtained by revisiting the procedure used to define the dynamic Clark model. Section IV will be thus devoted to the formulation of a new dynamic procedure for this model.

IV. A NEW DYNAMIC PROCEDURE FOR THE CLARK MODEL

A. A dynamic procedure based on Taylor series expansions

The starting point of the new dynamic procedure is a Taylor series expansion of the filtering operation. This approach has already been used by several authors to derive the gradient model⁹ or to improve the modeling of the SGS scalar variance.¹⁴ Here, the method to give an expansion for \bar{f} as function of \bar{f} and \bar{g} (where f and g are quantities describing flow fields) is briefly recalled (see Bedford and Yeou²⁵ for details).

In spectral space, the filtering operation is

$$\check{f}(\vec{k}) = \check{G}(\vec{k}) \check{f}(\vec{k}), \quad (17)$$

where $\check{f}(\vec{k})$ is the Fourier transform of $f(\vec{x})$ and \vec{k} is the wave vector. Considering a Gaussian filter, the kernel of this filter is given in spectral space by

$$\check{G}(\vec{k}) = \exp\left(-\frac{\bar{\Delta}^2}{24} k^2\right), \quad (18)$$

which can be expanded as Taylor series (writing only the first term),

$$\check{G}(\vec{k}) = 1 - \frac{\bar{\Delta}^2}{24} k^2 + \mathcal{O}(\bar{\Delta}^4). \quad (19)$$

Thus, the filtering operation (17) can be rewritten as

$$\check{f}(\vec{k}) = \check{f}(\vec{k}) - \frac{\bar{\Delta}^2}{24} k^2 \check{f}(\vec{k}) + \mathcal{O}(\bar{\Delta}^4). \quad (20)$$

Writing now the Laplacian operator $\mathcal{L}(f) = \partial^2 f / \partial x_i^2$, the inverse Fourier transform of Eq. (20) leads to

$$\bar{f} = f + \frac{\bar{\Delta}^2}{24} \mathcal{L}(f) + \mathcal{O}(\bar{\Delta}^4). \quad (21)$$

Moreover, with similar considerations, the Taylor series expansion of the function f can be written in spectral space as

$$\check{f}(\vec{k}) = \check{f}(\vec{k}) + \frac{\bar{\Delta}^2}{24} k^2 \check{f}(\vec{k}) + \mathcal{O}(\bar{\Delta}^4). \quad (22)$$

This allows to write

$$f = \bar{f} - \frac{\bar{\Delta}^2}{24} \mathcal{L}(\bar{f}) + \mathcal{O}(\bar{\Delta}^4), \quad (23)$$

in the physical space.

Now, writing Eq. (21) for the product function fg ,

$$\bar{fg} = fg + \frac{\bar{\Delta}^2}{24} \mathcal{L}(fg) + \mathcal{O}(\bar{\Delta}^4), \quad (24)$$

and using the Eq. (23) to replace f and g allows to write

$$\bar{fg} = \bar{f}\bar{g} + \frac{\bar{\Delta}^2}{12} \frac{\partial \bar{f}}{\partial x_j} \frac{\partial \bar{g}}{\partial x_j} + \mathcal{O}(\bar{\Delta}^4). \quad (25)$$

If only the first term of the RHS is considered, the gradient model is obtained. This development has been done for the Gaussian filter but it is also valid for the box filter. In fact, it can be proven that all symmetric, non-negative filters can be written as a convergent Taylor series.²⁷ However, note that the Taylor series expansion of the spectral cut-off filter leads to divergent series because of its non-localness.³ For this reason, it will be important to validate the model based on these relations when a spectral cut-off filter is used.

Now, instead of neglecting the other higher order terms, we propose to model these terms by $C_c \phi(\bar{\Delta}, \bar{f}, \bar{g})$, where C_c is a coefficient to define. Equation (25) is then written as

$$\overline{fg} - \bar{f}\bar{g} = \frac{\bar{\Delta}^2}{12} \frac{\partial \bar{f}}{\partial x_j} \frac{\partial \bar{g}}{\partial x_j} + C_c \varphi(\bar{\Delta}, \bar{f}, \bar{g}). \quad (26)$$

This formulation is equivalent to a Clark model where φ is the model used to stabilize the gradient model. Thus the Clark model of the SGS scalar flux, Eq. (10), can be written, choosing $f = u_i$, $g = Z$ and φ being the Smagorinsky-type model.

Since the previous operations depend only of the filter, the same consideration can now be done at the test filter level, leading to

$$\widehat{fg} - \widehat{f}\widehat{g} = \frac{\widehat{\Delta}^2}{12} \frac{\partial \widehat{f}}{\partial x_j} \frac{\partial \widehat{g}}{\partial x_j} + C_c \varphi(\widehat{\Delta}, \widehat{f}, \widehat{g}), \quad (27)$$

assuming the same coefficient, C_c , and the same functional form, φ , to model the higher order terms. Taking $f = \bar{u}_i$, $g = \bar{Z}$, and φ being the Smagorinsky-type model, Eq. (27) writes as

$$\widehat{\bar{u}_i \bar{Z}} - \widehat{\bar{u}_i} \widehat{\bar{Z}} = \frac{\widehat{\Delta}^2}{12} \frac{\partial \widehat{\bar{u}_i}}{\partial x_j} \frac{\partial \widehat{\bar{Z}}}{\partial x_j} + C_c \widehat{\Delta}^2 \left| \widehat{S} \right| \frac{\partial \widehat{\bar{Z}}}{\partial x_i}. \quad (28)$$

This defines a relation between the Leonard-type term, $\widehat{\bar{u}_i \bar{Z}} - \widehat{\bar{u}_i} \widehat{\bar{Z}}$, and other quantities available in LES. This relation can thus be used to compute the model coefficient C_c . Assuming C_c constant over homogeneous directions, it can be evaluated from a least-squares approximation according to Lilly's method.²¹ The new dynamic procedure is now defined as

$$C_c = \frac{\langle (L_i - K_i) N_i \rangle}{\langle N_i N_i \rangle}, \quad (29)$$

where L_i is the Leonard-type term, Eq. (7), $K_i = \frac{\widehat{\Delta}^2}{12} \frac{\partial \widehat{\bar{u}_i}}{\partial x_j} \frac{\partial \widehat{\bar{Z}}}{\partial x_j}$ and $N_i = \widehat{\Delta}^2 \left| \widehat{S} \right| \frac{\partial \widehat{\bar{Z}}}{\partial x_i}$. This defines the new proposed dynamic Clark model, referred as NDCM in the following. Note that this new dynamic procedure is easy to implement from the classic dynamic procedure (13), because it corresponds only to the suppression of the second term of the RHS in Eq. (8) and Eq. (12).

B. Relation between Germano's identity and the proposed dynamic procedure

The classic dynamic procedure recalled by Eq. (4) to (8) (for the Smagorinsky model) is based on the Germano's identity,

$$\widehat{\bar{u}_i \bar{Z}} - \widehat{\bar{u}_i} \widehat{\bar{Z}} = \widehat{\bar{u}_i \bar{Z}} - \widehat{\bar{u}_i} \widehat{\bar{Z}} - \left(\widehat{\bar{u}_i \bar{Z}} - \widehat{\bar{u}_i} \widehat{\bar{Z}} \right). \quad (30)$$

This relation (30) being exact, it is important to show that the new proposed dynamic procedure stays consistent with this identity. The two terms of the right-hand-side of Eq. (30) are thus evaluated from the Taylor series expansions (26) and (27). Writing the Taylor series expansion of the bar filter for the term $\widehat{\bar{u}_i \bar{Z}}$ by taking $f = u_i$ and $g = Z$ in Eq. (26) leads first to

$$\widehat{\bar{u}_i \bar{Z}} = \widehat{\bar{u}_i} \widehat{\bar{Z}} + \frac{\bar{\Delta}^2}{12} \frac{\partial \widehat{\bar{u}_i}}{\partial x_j} \frac{\partial \widehat{\bar{Z}}}{\partial x_j} + C_c \widehat{\varphi}(\bar{\Delta}, \widehat{\bar{u}_i}, \widehat{\bar{Z}}). \quad (31)$$

This first relation leads to an evaluation of the second term of the right-hand-side of Eq. (30), $\widehat{\bar{u}_i \bar{Z}} - \widehat{\bar{u}_i} \widehat{\bar{Z}}$. Note that the same result will be obtained with the first step of the classic dynamic procedure. Now, in the relation (31), replacing the term $\widehat{\bar{u}_i \bar{Z}}$ by the Taylor series expansion of the test filter (Eq. (27) with $f = \bar{u}_i$ and $g = \bar{Z}$) leads to

$$\widehat{\bar{u}_i \bar{Z}} = \widehat{\bar{u}_i} \widehat{\bar{Z}} + \frac{\widehat{\Delta}^2}{12} \frac{\partial \widehat{\bar{u}_i}}{\partial x_j} \frac{\partial \widehat{\bar{Z}}}{\partial x_j} + C_c \varphi(\widehat{\Delta}, \widehat{\bar{u}_i}, \widehat{\bar{Z}}) + \frac{\bar{\Delta}^2}{12} \frac{\partial \widehat{\bar{u}_i}}{\partial x_j} \frac{\partial \widehat{\bar{Z}}}{\partial x_j} + C_c \widehat{\varphi}(\bar{\Delta}, \widehat{\bar{u}_i}, \widehat{\bar{Z}}). \quad (32)$$

This relation leads thus to an evaluation of the first term of the right-hand-side of Eq. (30), $\widehat{\bar{u}_i \bar{Z}} - \widehat{\bar{u}_i} \widehat{\bar{Z}}$. Thus, by subtracting Eq. (31) from Eq. (32) and by taking φ as the Smagorinsky-type model, the relation (28) defining the new proposed dynamic procedure is found. In other words, the classic and the new proposed dynamic procedures for the Clark model differ only from the evaluation of the term $\widehat{\bar{u}_i \bar{Z}} - \widehat{\bar{u}_i} \widehat{\bar{Z}}$ in the Germano's identity. Indeed, for the classic dynamic procedure, this term is evaluated with the assumption that the Clark model can be used with the same model coefficient for the filter given by the combination of bar and test filters. Conversely, for the proposed dynamic procedure, this term is evaluated by using Taylor series expansions for both filters successively.

For completeness, a comparison between the coefficients computed from the classic and the new proposed dynamic procedure is performed. These coefficients are also compared with an "exact" coefficient computed from the DNS data. Indeed, from Eq. (10) and using a least-squares approximation, a "exact" coefficient can be defined as

$$C_c = \frac{\langle (T_i - Q_i) P_i \rangle}{\langle P_i P_i \rangle}, \quad (33)$$

where $Q_i = \frac{\bar{\Delta}^2}{12} \frac{\partial \bar{u}_i}{\partial x_j} \frac{\partial \bar{Z}}{\partial x_j}$ and $P_i = \bar{\Delta}^2 \left| \bar{S} \right| \frac{\partial \bar{Z}}{\partial x_i}$. Figure 5 shows the evolution of these coefficients with the filter width. As expected, the "exact" coefficient is not constant with the filter width even in such simple flow. This shows that a dynamic procedure is required for accurate predictions. Figure 5 shows also that the new proposed dynamic procedure leads to better agreement with the "exact" coefficient. Indeed, this procedure allows to decrease the large over-prediction of the coefficient magnitude due to the classic dynamic procedure. Better performance can thus be expected for NDCM.

C. Performance of the NDCM

The NDCM performances are now measured and compared with the dynamic Smagorinsky-type and the dynamic Clark models. To ensure that the model performance is not dependent on the filter kernel, the performances are measured for the box and spectral cut-off filters. Indeed, as

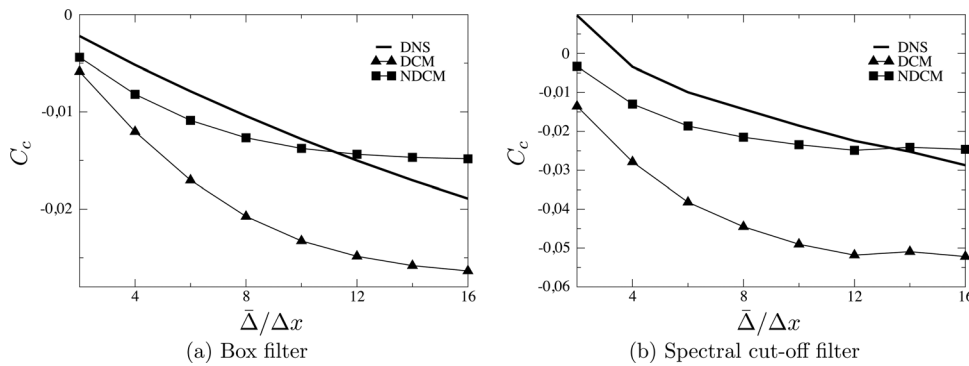


FIG. 5. Evolution of the Clark model coefficients with the filter width. The coefficients are evaluated from the classic dynamic procedure, Eq. (13), the new proposed dynamic procedure, Eq. (29), and from the DNS field, Eq. (33).

already written, the Taylor series expansion is formally valid for box and Gaussian filters but not for spectral cut-off filter. It is then important to validate the new dynamic procedure for this filter. Again, the optimal estimation analysis is performed to evaluate the capacity of the new model to accurately predict the divergence of the SGS scalar flux, $\partial T_i/\partial x_i$, and the SGS scalar dissipation, $T_i\partial\bar{Z}/\partial x_i$. Figures 6 and 7 show the comparison of the model errors. Note that NDCM and DCM have the same irreducible errors because these models are based on the same set of variables. The NDCM quadratic errors are the smallest quadratic errors in all the cases, showing the improvement allowed by the new dynamic procedure. In particular, the NDCM quadratic error on the SGS scalar dissipation for the spectral cut-off filter is much smaller than the DCM one (Fig. 7(b)). This shows an important improvement of the functional performance of the Clark model. Moreover, in all the cases, the NDCM quadratic errors stay close to their irreducible errors, showing that an improvement of the model cannot be performed without adding new variables. Finally, the NDCM quadratic errors are smaller than the DSM irreducible errors for both the SGS scalar flux and the SGS scalar dissipation. This means that any improvement of the Smagorinsky model (without new variable) will reach the structural and functional performances of NDCM.

The functional performance can also be studied at a global view. Figure 8 shows the evolution of the mean SGS scalar dissipation with the filter width. The improvement of the functional performance of the model implies a decreasing of the important over-prediction of the SGS scalar dissipation magnitude observed with DCM. Thus, the global SGS scalar dissipation predicted by the new model (NDCM) stays close to the DNS results, whereas DCM is even more dissipative than DSM.

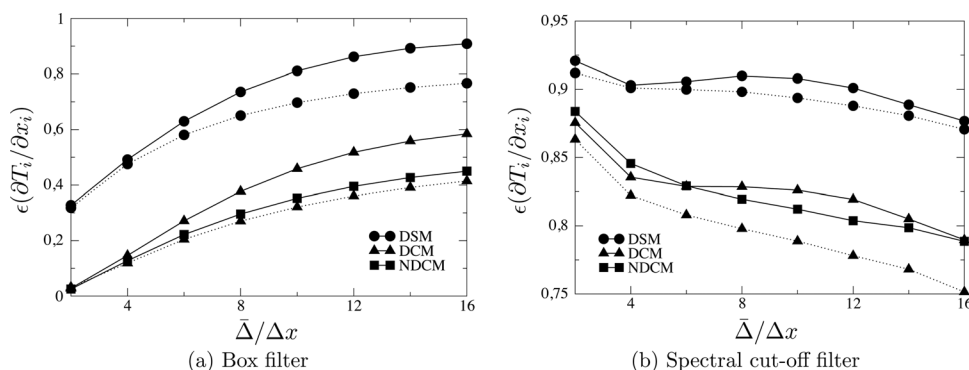


FIG. 6. Evolution of the quadratic errors (solid line) of the models on the prediction of $\partial T_i/\partial x_i$ and their associated irreducible errors (dotted line) with the filter width.

V. A POSTERIORI (LES) TESTS

A. Description of the LES test case

The new model for T_i has been implemented and is now tested by performing LES. In this test case, only the scalar is solved by LES. The velocity field is still solved by DNS. Thus, at each time step, the velocity field is extrapolated from the DNS to the LES mesh in spectral space. This spectral extrapolation is equivalent to a spectral cut-off filter. The resulting filtered velocity field is then used to advance the filtered scalar field. The advantage of this procedure is that no SGS model is needed for the Navier-Stokes equations and there is then no modeling error on the velocity field used in the filtered scalar equation. Thus, when the LES data are compared with the filtered DNS data, the difference will be only due to the model used for the SGS scalar flux.

The numerical methods and the flow configuration are similar to the ones described in Sec. II. The velocity field is still resolved on 512^3 grid points. Two LES meshes are used to investigate the performance of the models: 64^3 and 32^3 grid points. Moreover, to instigate the models performance as a function of the molecular Schmidt number, two other types of LES are performed for $Sc = 0.2$ and $Sc = 5.0$ on a mesh composed by 64^3 grid points. In all the LES, the initial scalar field is obtained by spectral extrapolation of the initial DNS scalar field to the LES mesh. Various LES are performed using DSM, DCM, and NDCM as SGS model. All these LES will be compared with the results of a 512^3 grid points DNS, except for the case with $Sc = 5.0$. Indeed, in this case, the Batchelor scale is too small to be able to perform a DNS with a mesh composed by 512^3 grid points. The results will be thus compared with a well-resolved 512^3 grid points LES using NDCM as SGS scalar flux model for this case.

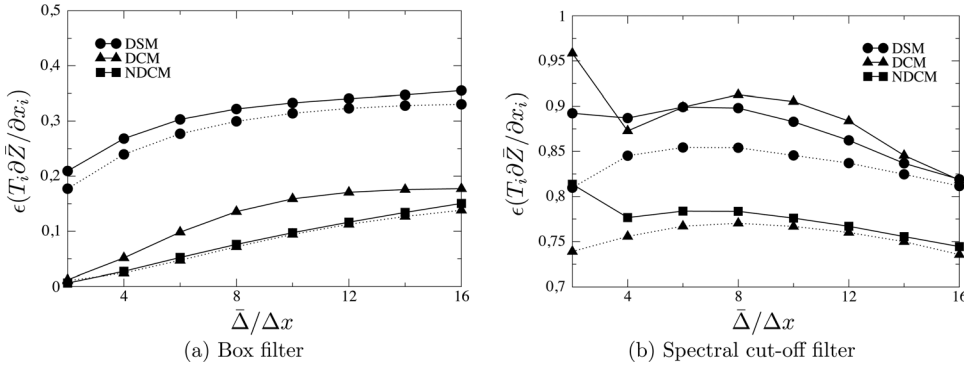


FIG. 7. Evolution of the quadratic errors (solid line) of the models on the prediction of $T_i \partial \bar{Z} / \partial x_i$ and their associated irreducible errors (dotted line) with the filter width.

Note, however, that this well-resolved LES is denoted as “DNS” below for convenience. Since spectral method is used in these tests, the implicit filtering is equivalent to a spectral cut-off filter. The LES results will be then compared with the DNS filtered results using a spectral cut-off filter. Note that the LES cases solved on 64^3 and 32^3 grid points, for $Sc = 1.0$, are compared with the same DNS database. Only the width in the filtering operation of the DNS data is changed in these cases. As already explained, this is a severe test case since the Taylor series expansions, which are the starting point of the new procedure, are formally valid only for symmetric and non-negative filters.

B. LES results

To first compare the LES performed, Figure 9 shows the time evolution of the LES resolved scalar variance, $\langle \bar{Z}^2 \rangle = \langle \bar{Z} \bar{Z} \rangle - \langle \bar{Z} \rangle \langle \bar{Z} \rangle$. The LES resolved scalar variance is compared with the variance of the filtered scalar computing from a spectral cut-off filtering of the DNS data. Moreover, DNS (no-filtered) scalar variance, $\langle Z'^2 \rangle = \langle Z^2 \rangle - \langle Z \rangle^2$, is also shown. The filtered DNS scalar variance is always smaller than the DNS (no-filtered) scalar variance because the fluctuations smaller than the filter width are not taken into account. The gap between the filtered DNS scalar variance and the DNS scalar variance is thus higher for higher filter width (Figs. 9(a) and 9(b)) but also for higher Schmidt number because the range of small scales is broader with a smaller Batchelor scale (Figs. 9(a) and 9(d)). Conversely, the difference between the filtered DNS scalar variance and the DNS scalar variance is not visible for the case with $Sc = 0.2$ because the Batchelor scale is larger for this case and the part due to subfilter scales is negligible (Fig. 9(c)). The DCM

resolved scalar variance is always strongly smaller than the filtered DNS scalar variance. This is because DCM over-predicts the transfer between the resolved scales and the sub-grid scales. This behavior was already found in the *a priori* tests, when the over-dissipation of DCM for a spectral cut-off filter was observed. As expected, the new dynamic procedure (NDCM) allows to correct this behavior with a weaker over-prediction of the decreasing of the resolved scalar variance. Finally, NDCM leads generally to similar or better agreement with the filtered DNS than DSM. In particular, DSM predicts a large over-dissipation similar to DCM for the some cases: $Sc = 1.0$ and $Sc = 5.0$ with 64^3 grid points.

For further analysis, the scalar variance spectrum (Figure 10) and the scalar probability density function (PDF, Figure 11) are computed at $t = 0.1$. This time corresponds roughly to a mixing state close to the equipartition of the scalar value on a range from 0 to 1 for the DNS results (see Figure 11). As shown by Fig. 10, DSM and DCM under-predict the scalar variance spectrum at the smallest resolved scales (highest resolved wave numbers), whereas NDCM stays close to the DNS at all the resolved scales. For DCM, this is due to the over-prediction of the global SGS scalar dissipation, whereas for DSM, this is probably due to an incorrect prediction of the local SGS scalar dissipation. Indeed, for some cases ($Sc = 1.0$ on 32^3 grid points, for example), the global SGS scalar dissipation predicted by DSM is similar to the global SGS scalar dissipation predicted by NDCM with the same variance decrease (Fig. 9(b)). However, the *a priori* tests had shown a weak local functional performance for DSM with a large quadratic error on the prediction of the SGS scalar dissipation in comparison with NDCM (Fig. 7). This is what is found again in these *a posteriori* tests with the comparison of the scalar variance spectrum. Note that

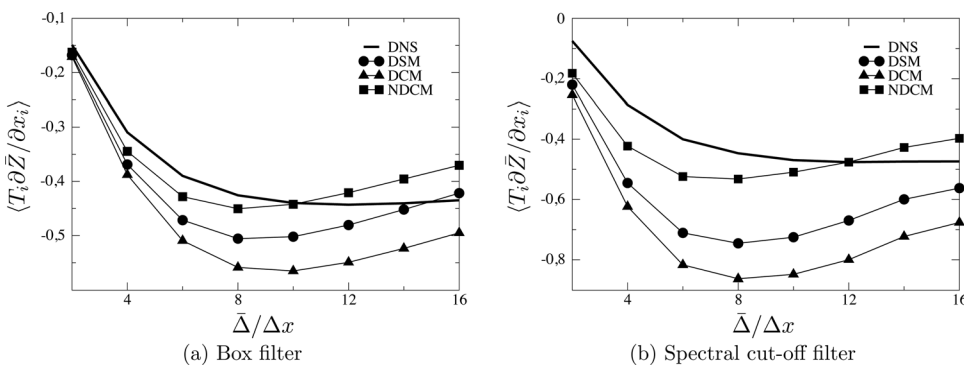


FIG. 8. Evolution of the mean SGS scalar dissipation, $\langle T_i \partial \bar{Z} / \partial x_i \rangle$, with the filter width.

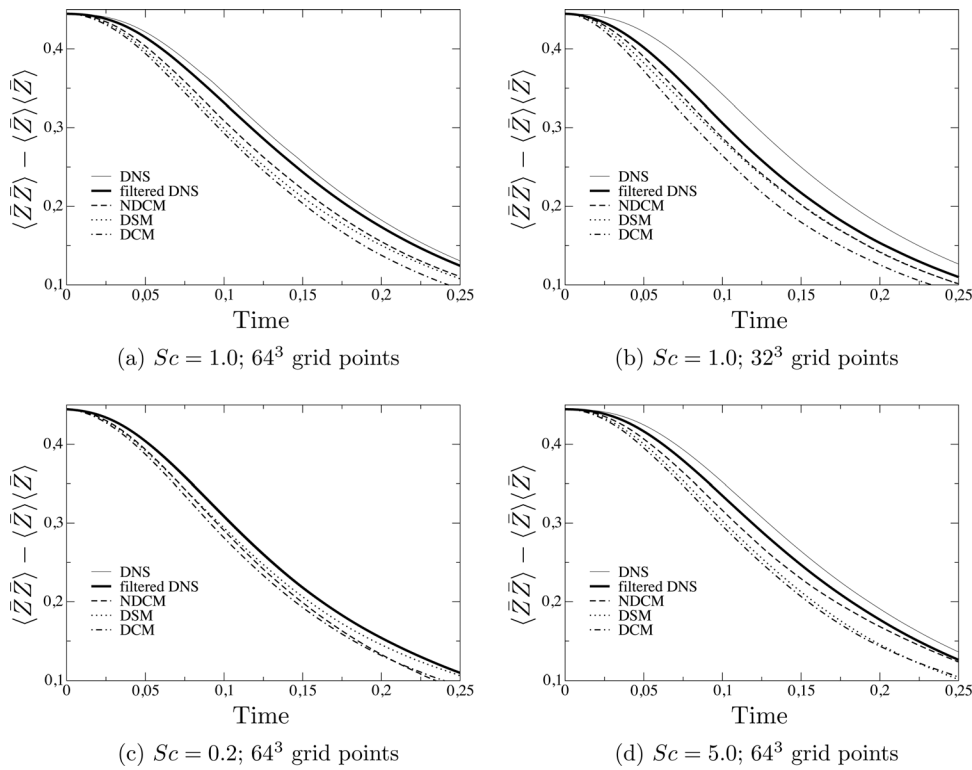


FIG. 9. Evolution of the LES resolved scalar variance, $\langle \bar{Z}^2 \rangle$, with time. The filtered and no-filtered DNS scalar variances are also shown for comparison.

this point underlines that a comparison of global SGS scalar dissipations in *a priori* tests is not enough to understand the model performance, and that measurements of local performance (as performed with the quadratic errors analysis) are also needed. The SGS scalar flux model performance will have consequences on the local mixing prediction as it can be observed with the scalar PDF (Figure 11). Thus, the over-

prediction of the SGS scalar dissipation due to DCM and DSM implies an over-prediction of the mixing. As consequences, the part of unmixed fluid, $\bar{Z} \approx 0$ or $\bar{Z} \approx 1$, is under-predicted with smaller PDF values than the filtered DNS, whereas the part of fully mixed fluid, $\bar{Z} \approx 0.5$, is over-predicted with higher PDF values than the filtered DNS. NDCM also over-predicts the mixing, but the over-

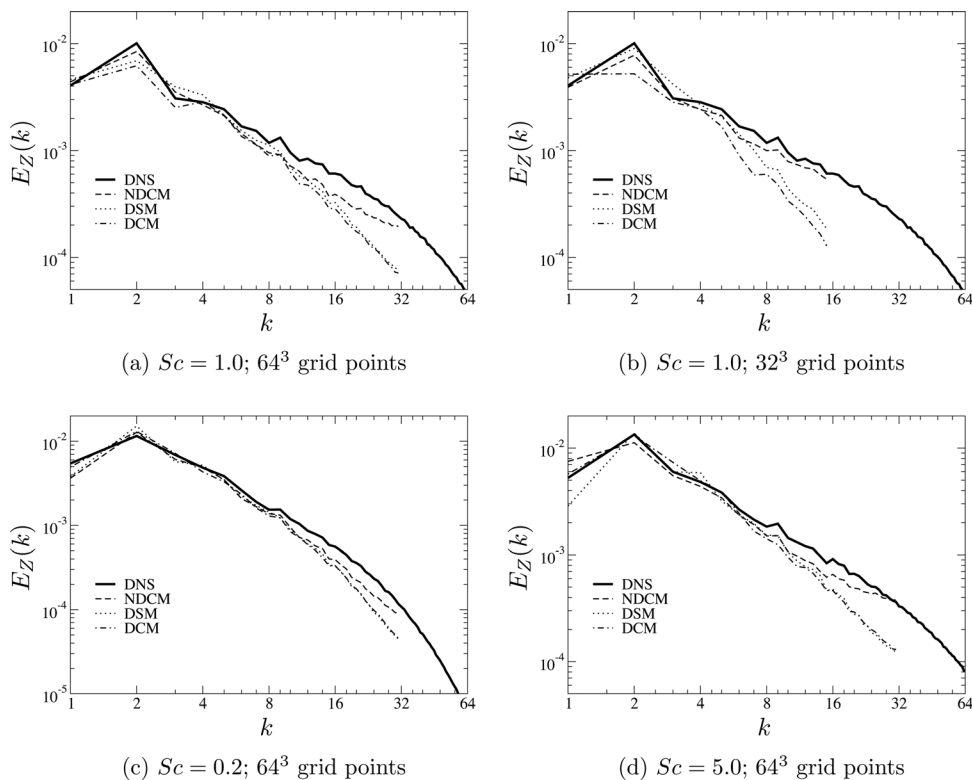


FIG. 10. Scalar variance spectrum, $E_Z(k)$ at $t = 0.1$.

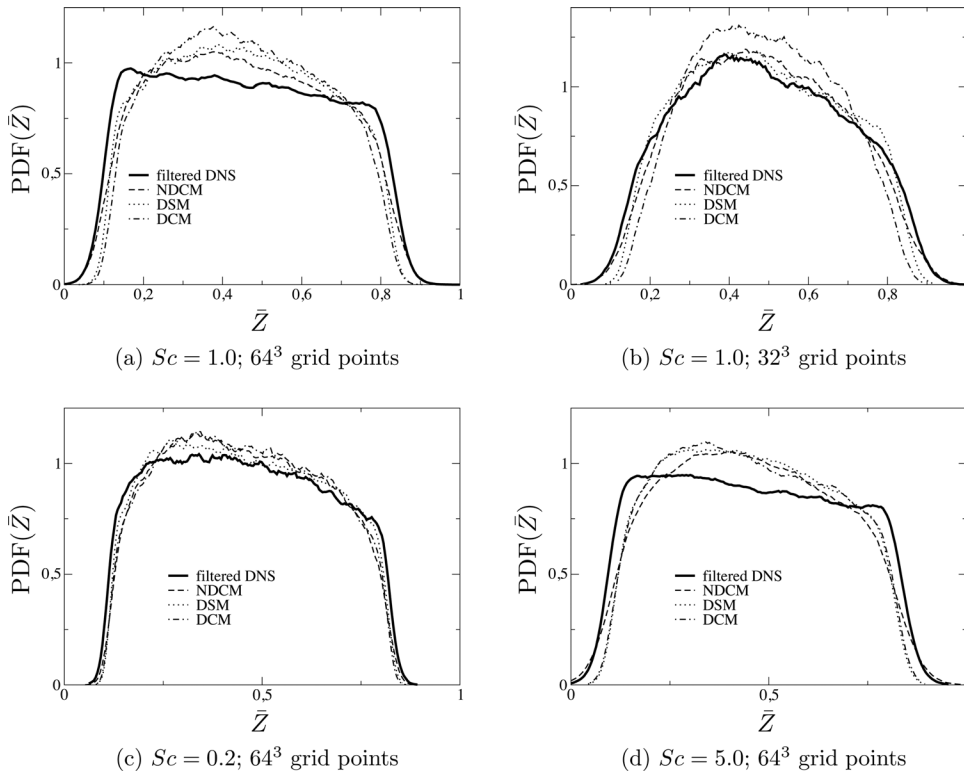


FIG. 11. PDF of the LES resolved scalar at $t = 0.1$. The PDF of the DNS filtered scalar is also shown for comparison.

prediction is weaker. In particular, the part of unmixed fluid is better predicted than with DCM and DSM.

Finally, the influence of the SGS scalar flux model on the time correlation of the LES resolved scalar can be studied. Indeed, subgrid-scales contribute to temporal decorrelation of the resolved scales. The SGS model has thus to lead to a correct temporal decorrelation to reproduce correct

subgrid scales effects.²⁸ The time auto-correlation of the LES resolved scalar is defined as

$$C_{(\bar{Z})}(t) = \frac{\langle \bar{Z}'(\vec{x}, t_0) \bar{Z}'(\vec{x}, t) \rangle}{(\langle \bar{Z}'^2(\vec{x}, t_0) \rangle \langle \bar{Z}'^2(\vec{x}, t) \rangle)^{1/2}}, \quad (34)$$

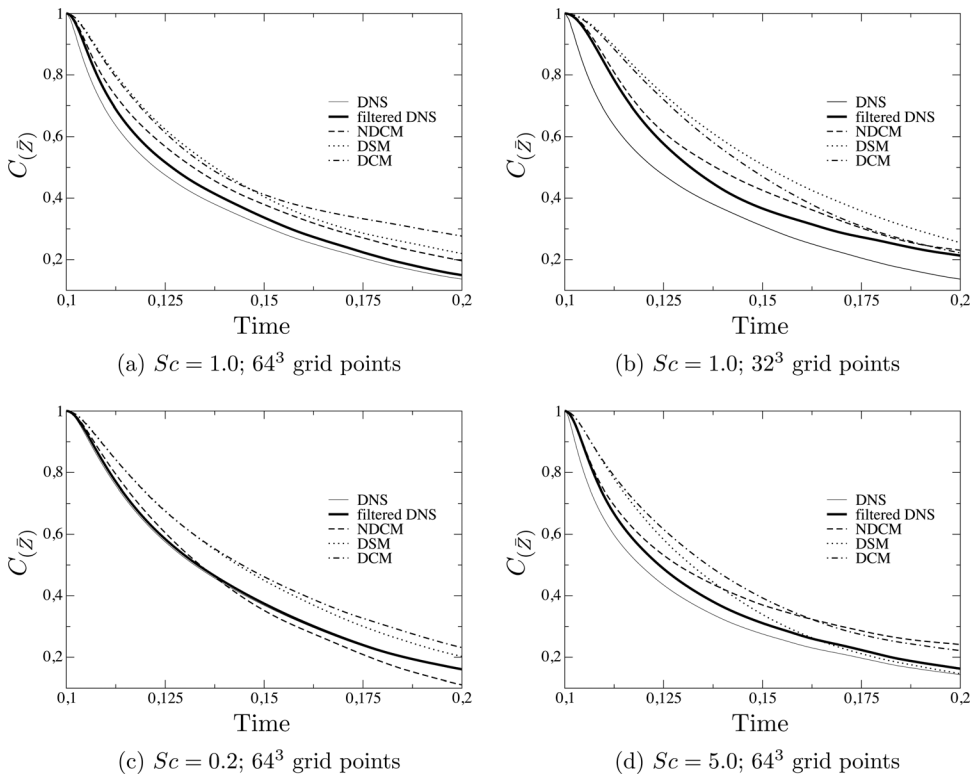


FIG. 12. Time correlation of the LES resolved scalar, $C_{(\bar{Z})}$, computed by Eq. (34). The correlation computed from the filtered and no-filtered DNS scalar is also shown for comparison.

where \bar{Z}' is the scalar fluctuation field. Figure 12 shows the evolution of $C(\bar{Z})$ for the different LES. The correlation has been computed taking $t_0 = 0.1$, i.e., when the scalar field is close to the equipartition of the scalar value on a range from 0 to 1. The time correlation for filtered and no-filtered DNS data is also shown for comparison. The time correlation of the filtered DNS data stays always higher than the time correlation of the no-filtered DNS data. This is because only the large scales are taken into account when the time correlation is computed with the filtered DNS data and these large scales are known to be better correlated than small scales. Note that the difference between filtered and no-filtered DNS data is not visible for $Sc = 0.2$ because the part of subfilter scales is reduced in this case. NDCM seems to lead to better agreement with the filtered DNS data. Indeed, DCM and DSM lead to higher correlations whereas NDCM predicts faster decorrelation than the other models at the beginning. This is probably due to a better prediction of the mixing activities at the smallest resolved scales, as already shown by studying scalar variance spectra. Thus, the smallest resolved scales contribution to temporal decorrelation is better reproduced by NDCM than by DCM and DSM. In future works, further analysis could be carried out by studying two-points time correlations,²⁸ as well as Lagrangian time correlations.²⁹

VI. CONCLUSION

The SGS scalar flux model was evaluated using the concept of optimal estimators. This allows to measure the structural and functional performances of SGS models. It appears more suitable to formulate a SGS scalar flux model by using a dynamic Clark model approach. However, it was found that the classic dynamic procedure used with the Clark model leads to large errors in the predictions. Indeed, the dynamic Clark model shows a better correlation with the DNS than the dynamic Smagorinsky model, but it has a low accuracy to model the subgrid-scale scalar dissipation. Thus, it appears that the dynamic procedure used is not fully optimized. Starting from Taylor series expansions, a new dynamic model formulation is proposed. *A priori* tests of homogeneous isotropic turbulence showed that the new model substantially improves the predictive accuracy. This is confirmed by *a posteriori* tests where the new model is implemented and where various scalar statistic quantities are compared with filtered DNS results.

ACKNOWLEDGMENTS

This work is supported by the Agence Nationale pour la Recherche (ANR) under Contract No. ANR-2010-JCJC-091601. Computing resources were provided by IDRIS-CNRS.

¹M. Lesieur and O. Métais, "New trends in large-eddy simulations of turbulence," *Ann. Rev. Fluid Mech.* **28**, 45 (1996).

²C. Meneveau and J. Katz, "Scale-invariance and turbulence models for large-eddy simulation," *Ann. Rev. Fluid Mech.* **28**, 45 (2001).

³P. Sagaut, *Large Eddy Simulation for Incompressible Flows: An Introduction* (Springer, Berlin, 2006).

⁴C. Brun, G. Balarac, C. B. da Silva, and O. Métais, "Effects of molecular diffusion on the subgrid-scale modelling of passive scalars," *Phys. Fluids* **20**(2), 025102 (2008).

⁵D. You and P. Moin, "A dynamic global-coefficient subgrid-scale model for large-eddy simulation of turbulent scalar transport in complex geometries," *Phys. Fluids* **21**, 045109 (2009).

⁶M. Lesieur and R. Rogallo, "Large eddy simulation of passive scalar diffusion in isotropic turbulence," *Phys. Fluids A* **1**(9), 718 (1989).

⁷O. Métais and M. Lesieur, "Spectral large-eddy simulation of isotropic and stably stratified turbulence," *J. Fluid Mech.* **239**, 157 (1992).

⁸P. Moin, K. Squires, W. Cabot, and S. Lee, "A dynamic subgrid-scale model for compressible turbulence and scalar transport," *Phys. Fluids A* **3**, 2746 (1991).

⁹R. A. Clark, J. H. Ferziger, and W. C. Reynolds, "Evaluation of subgrid-scale models using an accurately simulated turbulent flow," *J. Fluid Mech.* **91**, 1 (1979).

¹⁰B. Vreman, B. Geurts, and H. Kuerten, "Large-eddy simulation of the turbulent mixing layer," *J. Fluid Mech.* **339**, 357 (1997).

¹¹K. Alvelius, "Random forcing of three-dimensional homogeneous turbulence," *Phys. Fluids* **11**, 1880 (1999).

¹²V. Eswaran and S. B. Pope, "Direct numerical simulations of the turbulent mixing of a passive scalar," *Phys. Fluids* **31**, 506 (1988).

¹³S. B. Pope, *Turbulent Flows* (Cambridge University Press, New York, 2000).

¹⁴G. Balarac, H. Pitsch, and V. Raman, "Development of a dynamic model for the subfilter scalar variance using the concept of optimal estimators," *Phys. Fluids* **20**(3), 035114 (2008).

¹⁵G. Balarac, H. Pitsch, and V. Raman, "Modeling of the subfilter scalar dissipation rate using the concept of optimal estimators," *Phys. Fluids* **20**(9), 091701 (2008).

¹⁶C. M. Kaul, V. Raman, G. Balarac, and H. Pitsch, "Numerical errors in the computation of subfilter scalar variance in large eddy simulations," *Phys. Fluids* **21**(5), 055102 (2009).

¹⁷R. S. Rogallo and P. Moin, "Numerical simulation of turbulent flows," *Ann. Rev. Fluid Mech.* **16**, 99 (1984).

¹⁸U. Schumann, "Subgrid scale model for finite difference simulations of turbulent flows in plane channels and annuli," *J. Comput. Phys.* **404**, 376 (1975).

¹⁹J. Smagorinsky, "General circulation experiments with the primitive equations," *Mon. Weather Rev.* **91**, 99 (1963).

²⁰M. Germano, U. Piomelli, P. Moin, and W. H. Cabot, "A dynamic subgrid-scale eddy viscosity model," *Phys. Fluids A* **3**, 1760 (1991).

²¹D. K. Lilly, "A proposed modification of the Germano subgrid-scale closure method," *Phys. Fluids A* **4**, 633 (1992).

²²R. Deutsch, *Estimation Theory* (Prentice-Hall, Englewood Cliffs, NJ, 1965).

²³A. Moreau, O. Teytaud, and J. P. Bertoglio, "Optimal estimation for large-eddy simulation of turbulence and application to the analysis of subgrid models," *Phys. Fluids* **18**, 105101 (2006).

²⁴J. A. Langford and R. D. Moser, "Optimal LES formulations for isotropic turbulence," *J. Fluid Mech.* **398**, 321 (1999).

²⁵K. W. Bedford and W. K. Yeo, "Conjunctive filtering procedures in surface water flow and transport," in *Large Eddy Simulation of Complex Engineering and Geophysical Flows*, edited by B. Galperin and S. A. Orszag (Cambridge University Press, New York, 1993).

²⁶B. Vreman, B. Geurts, and H. Kuerten, "Large eddy simulation of the temporal mixing layer using the Clark model," *Theor. Comput. Fluid Dyn.* **8**, 309 (1996).

²⁷C. D. Pruett, J. S. Sochacki, and N. A. Adams, "On Taylor-series expansions of residual stresses," *Phys. Fluids* **13**, 32578 (2001).

²⁸G. W. He, R. Rubinstein, and L.-P. Wang, "Effects of subgrid-scale modeling on time correlations in large eddy simulation," *Phys. Fluids* **14**, 3186 (2002).

²⁹Y. Yang, G. W. He, and L.-P. Wang, "Effects of subgrid-scale modeling on Lagrangian statistics in large eddy simulation," *J. Turbul.* **9**, 1 (2008).